Research Square

Preprints are preliminary reports that have not undergone peer review.
They should not be considered conclusive, used to inform clinical practice,
or referenced by the media as validated information.

Major Long-term Shifts in Spatial and Annual Plankton Biodiversity Patterns in the North Atlantic Ocean

Jérôme Castant

jerome.castant@outlook.com

Laboratoire d'Océanologie et de Géosciences https://orcid.org/0009-0003-8758-5805

Vincent Vantrepotte

Laboratoire d'Océanologie et de Géosciences, Université du Littoral Côte d'Opale, Université Lille

Philip Reid

The Marine Biological Association https://orcid.org/0000-0001-7728-6746

Grégory Beaugrand

Univ. Littoral Côte d'Opale, CNRS, Univ. Lille, UMR 8187 LOG https://orcid.org/0000-0002-0712-5223

Biological Sciences - Article

Keywords: Plankton, Marine biodiversity, Phenology, Climate change, Long-term trends, Ecosystem functioning

Posted Date: March 3rd, 2026

DOI: https://doi.org/10.21203/rs.3.rs-8252199/v1

License: This work is licensed under a Creative Commons Attribution 4.0 International License.
Read Full License

Additional Declarations: There is **NO** Competing Interest.

Abstract

Despite the fundamental role played by marine biodiversity within ecosystem functions and services, the impacts of climate on this key ecosystem property remain poorly documented. Here, we investigate long-term changes in spatial and annual biodiversity patterns for three key plankton groups (diatoms, dinoflagellates, and copepods) across the North Atlantic over ~ 6 decades (1958–2022) at a high spatio-temporal resolution. Over this period we show that biodiversity has generally increased polewards, with significant positive trends that cover ~ 30% [27; 38.9%] of the basin area for all three groups. Between the cold 1965–1985 and warm 2002–2022 periods, mean biodiversity has increased by ~ 8–17% [4.4; 22.2%] in cold-water regions, associated with significant expansions of high-biodiversity periods by up to 21 days [9.48; 25.33]. This pronounced change in species phenology is likely to desynchronise trophic interactions within the ecological networks and perturb energy transfer from primary producers to higher trophic levels.

Main

Plankton monitoring provides a sensitive lens through which to explore, detect and interpret shifts in marine ecosystems[1]. As foundational components of pelagic food webs, plankton mediate key ecosystem functions, including trophic transfer, biogeochemical cycling, and carbon export[2,3]. Phytoplankton alone contribute approximately half of global net primary production, forming the base of marine food webs[4], while zooplankton facilitate the flow of this energy to higher trophic levels, including fish, marine mammals and seabirds[5,6]. Their short life cycles and high turnover rates make planktonic communities sensitive to environmental variability, which explains why they are key indicators of ecological change[7].

Climate change is altering plankton ecosystems and many biological responses have been identified, ranging from biogeographical to phenological shifts and long-term changes in abundance[8]. Biogeographical shifts have been documented as well and it is expected that marine biodiversity will reorganise as a result of climate change. Phenology (i.e., the study of the seasonal timing of biological events) and its alterations in space and time is also changing[9,10]. Shifts in phenology may not only influence productivity and nutrient cycling via taxon-specific uptake strategies[11], but also may modulate carbon export efficiency[12] and predator-prey synchrony, with implications for food web stability and resilience[13].

Previous research on plankton phenology has largely focused on shifts in biomass or abundance of key indicator species[9,14,15] but has rarely examined changes in the annual biodiversity patterns of key plankton groups. As plankton biodiversity emerges from complex ecological interactions that structure community dynamics across space and time[16,17], it is the maintenance of this interconnected biodiversity that supports ecosystem functioning, which in turn determine ecosystem services that underpin human well-being[18]. Plankton biodiversity is a fundamental property of marine ecosystems and

an indicator of ecosystem structure, stability and function. Changes in this property in space and time may have severe consequences at the ecosystem level.

Here, we reanalyse the largest plankton dataset in the world, the Continuous Plankton Recorder (CPR) survey[19], at a high spatial-temporal resolution (i.e. daily resolution, 0.25° latitude x 0.25° longitude) by using a new methodology (Methods)[20,21]. Our study investigates spatio-temporal changes in the biodiversity of three key taxonomic groups (diatoms, dinoflagellates, and copepods) at the scale of the North Atlantic with a focus on changes in annual biodiversity patterns at fine spatial and temporal scales.

Spatial and Temporal Trends in Plankton Richness

We applied a new procedure to reanalyse the CPR dataset at high spatial and temporal resolutions (see Methods). This procedure uses a recently developed model, the Environmental String Model (ESM), which assesses the niche of a species by means of environmental strings, preserving the local relationships among variables[20,22]. The procedure was performed at a species level for diatoms (46 species), dinoflagellates (26 species) and copepods (44 species, a total of 116 species), at a spatial resolution of 0.25° latitude x 0.25° longitude and at a daily resolution from 1958 to 2022 (23741 days; supplementary Table S1)[21]. We examined large-scale spatial changes in annual maximum species richness for the three groups as well as long-term changes in yearly means (Fig. 1). We selected a maximum instead of a simple mean to avoid misinterpretation by averaging over 365 days, but retained the mean for the Kendall analysis because it represents a more commonly applied measure of central tendency[23]. This first set of analyses was conducted to confirm that our approach reproduces previously reported spatial biodiversity patterns.

At a North Atlantic scale, the spatial distributions for maximum species richness are consistent with earlier studies[24,25] but for biodiversity (i.e. species richness, called biodiversity hereafter) the patterns reveal a much finer spatial structure, with clear influence of the Oceanic Polar Front for dinoflagellates and copepods (Supplementary Fig. S1a) and of bathymetry across the three groups (Supplementary Fig. S1b), consistent with the incorporation of bathymetry into our modelling framework (see methods). Maximum diatom biodiversity for example is highest on European shelves with a coastal-to-offshore gradient and closely follows major topographic features such as the Rockall Plateau, Reykjanes Ridge, Flemish Cap and the Vøring Plateau. Although also regionally influenced by continental shelf edges and deep basins, dinoflagellate biodiversity declines polewards. Bathymetry also shapes their distribution in a way that differs from diatoms, as relatively higher species richness is seen within eastern Atlantic deep-water features such as the Rockall Trough and Porcupine Seabight (Fig. 1b). Copepod biodiversity peaks south of the Oceanic Polar Front, at the northern edge of the Subtropical Gyre, and along the European shelf-edge (Fig. 1c).

Next, we examined long-term changes in mean annual biodiversity throughout the North Atlantic (Fig. 1d-f). Assessed by means of Kendall's τ (Methods), we found that long-term trends (1958-2022) are significantly (p-value < 0.05) positive (i.e. increase in biodiversity) for diatoms extending along the eastern Atlantic margin from northern Labrador Sea (~65° N) to ~40-45° N, encompassing the North Sea, Celtic Sea, Norwegian coasts, and the Grand Banks of Newfoundland. No significant trend occurs around the Flemish Cap region, where high short-term physical variability continually redistributes water masses[26], preventing consistent long-term changes in biodiversity from emerging. Positive trends represent 38.9% of the whole studied area (~5.38 × 10^6 km^2), while negative trends occur mainly in the eastern basin, representing 13.9% of the area (~1.93 × 10^6 km^2; Fig. 1d)[27]. Dinoflagellates exhibit widespread long-term increases in biodiversity across the western basin (Labrador Sea and Grand Banks of Newfoundland), the North Sea, and in some high latitudes, covering 35.4% of the whole studied area (~4.93 × 10^6 km^2), while localised declines are observed over 10.4% of the area (~1.44 × 10^6 km^2), particularly in the central southern oceanic area (Fig. 1e)[27,28]. The pattern of increase is similar to that of diatoms, extending from the Labrador Sea to the southernmost latitudes along the eastern Atlantic, with marked increases in the Norwegian Sea and along the northern boundary of the Subpolar gyre. Copepods exhibit positive trends across 27% of the whole studied area (~3.76 × 10^6 km^2), notably in the margins of the Subpolar Gyre, the North Sea and Norwegian Sea, but declines over 17.7% of the area (~2.45 × 10^6 km^2), mostly in polar seas and in a mid-Atlantic area, regions where diatom and dinoflagellate biodiversity increases (Fig. 1f)[29]. This analysis reveals significant biodiversity shifts across the North Atlantic and adjacent seas, characterised primarily by an increase in biodiversity.

Fine-Scale Changes in Annual Biodiversity Patterns Across the North Atlantic

We then investigate changes in the annual biodiversity patterns of the three taxonomic groups at a daily resolution in four representative regions of the North Atlantic (Fig. 2): (i) North-West Atlantic (NWA), (ii) North-East Atlantic (NEA), (iii) North Sea (NS) and (iv) Bay of Biscay (BSC, Methods); these regions follow a thermal gradient from short cool to long warm seasons (Fig. 2m-p); they also exhibit distinct bathymetry (Supplementary Fig. S1). Diatoms exhibit pronounced seasonality, with low biodiversity in winter and marked peaks in spring and summer, particularly in the cooler NWA and NEA (Fig. 2a-b, m). In warmer regions (NS, BSC), diatom biodiversity remains elevated for a longer period but displays a bimodal pattern, with distinct spring and late-summer peaks, consistent with their thermal preferences (Fig. 2c-d)[8]. Dinoflagellate biodiversity follows a similar latitudinal pattern, with a slightly narrower warm-season signal in the NWA and NEA, but a single (i.e. no bimodal pattern) extended period of high biodiversity from late spring to autumn in the NS and BSC (Fig. 2e-h). Copepods show weaker seasonality in the NWA, where biodiversity remains low throughout the year, consistent with overall low biodiversity in this region (Fig. 1c), but display a distinct seasonal pattern in the NEA with late summer/autumn maxima and show constant high biodiversity from spring to winter in the NS and BSC (Fig. 2i-l).

The four-region gradient may provide a natural analogue to help anticipate future biodiversity dynamics across taxa and systems. As global temperatures rise, thermal regimes are shifting polewards, altering annual biodiversity patterns[30]. In cooler ecosystems, biodiversity is expected to shift from short and sharp biodiversity peaks to more prolonged and stable periods of high biodiversity. However, as temperatures continue to rise they may become too high in certain locations and start to affect negatively the annual biodiversity patterns of some plankton groups[8]. These predictions are confirmed by Kendall's τ analysis, which reveals a significant temporal expansion (p-value < 0.05, thick black curves in Fig. 2) of the high-biodiversity periods for both diatoms and dinoflagellates in the cooler basins, indicating earlier spring onsets and later autumn declines consistent with longer warm seasons (Fig. 2a, e). These shifts imply that future conditions in the NWA may increasingly be comparable to the current annual biodiversity patterns observed in the NEA (Fig. 2b, f). In warmer regions, emerging summer declines in diatom biodiversity (BSC, Fig. 2d) and dinoflagellates (NS, Fig. 2g) suggest that temperature may already be approaching the upper thermal limits of these groups and constrain biodiversity. For diatoms, the patterns observed in the BSC may suggest that similar declines could emerge in the NS in the decades to come. However, the contrasting responses between the BSC (i.e. deep oceanic system) and the shallower NS (i.e. neritic system) for dinoflagellates suggest that differences in bathymetry may also lead to distinctly different annual biodiversity patterns. Similarly, while copepods show no clear temporal trends in the colder NWA, the seasonal duration of the high biodiversity period increases southwards. Some differences are observed between the NS and BSC, with late spring/summer declines in the NS) and earlier spring onsets and later autumn declines in the BSC (Fig. 2k *versus* Fig. 2l). This analysis highlights how spatial gradients may provide some guidelines against which changes in annual biodiversity patterns may be anticipated under climate warming.

Estimations of the alterations of annual biodiversity patterns

Estimating precisely the observed shifts in the annual biodiversity patterns is essential to anticipate their potential ecological implications. To this end, we used five indicators for each group and region (as previously used in phenology[31], Methods) to compare two time periods: 1965-1985, a relatively cool period in a negative phase of the Atlantic Multidecadal Variability index (AMV, ~8.82°C), and 2002-2022, a relatively warm period in a positive AMV phase (~9.14°C, Methods). The indicators are: (i) annual duration of the high-biodiversity period, (ii) onset, (iii) offset, (iv) day of Maximum Annual Richness (MAR) and (v) mean annual richness (vertical bars at the right side in Fig. 3). Visual assessments of these indicators for each year are provided in Supplementary Fig. S3. Results confirm the Kendall analysis performed in Fig. 2, with an overall expansion of the high-biodiversity (i.e. species richness) annual period in recent years due to earlier onsets and later offsets in most regions and groups, associated with higher mean biodiversity (Fig. 3). Along the thermal gradient, the strongest shifts in annual biodiversity patterns for diatoms and dinoflagellates occur in the coldest region (NWA), where the annual duration of the high-biodiversity period expanded by about 20 days [12.40; 26.86] (Supplementary Table S2), representing increases of +10.7% and +13.7% compared to the 1965-1985 period, respectively,

reflecting the high sensitivity of cold-water assemblages to warming[8]. These shifts are associated with a significant increase in mean biodiversity (Mann-Whitney U test, p-value < 0.05, Fig. 3a, e), corresponding to +8.7% and +17.2% for diatoms and dinoflagellates, respectively. Biodiversity shifts are more nuanced for both groups in the NEA, while copepods show significant expansion by ~15 days [9.48; 20.48] (+9%, Fig. 3j). In the NS, all three groups lengthen their high-biodiversity annual period by 8-13 days [4.10; 17.43] (Fig. 3c, g, k), though copepods adjust mainly through later offsets rather than earlier onsets (Fig. 3k), suggesting a decline in the thermal suitability of formerly dominant species and a shift toward taxa with autumn-dominant phenologies[23,32]. In the warmest region (BSC, Fig. 3d, h, l), diatoms deviate from the general pattern: later onset and earlier offsets significantly shorten their high-richness period by ~15 days [-22.43; -6.81] (-5.7%), associated with a decrease in mean biodiversity (-5.1%), both likely reflecting increasing summer thermal constraints. Copepods in contrast in the BSC expand their high-richness annual duration by ~8 days [6.48; 10.05] (+3.8%) and advance MAR by ~9 days [-11.43; -6.33], sustaining higher mean biodiversity, while dinoflagellates shift only in MAR, advancing by ~8 days [-12.24; -3.67].

Discussion

In this study, we show how the spatio-temporal biodiversity patterns of three key plankton groups have shifted in the North Atlantic, using a novel plankton reanalysis that combines long-term and high spatio-temporally resolved data[21]. Our approach reproduces well the spatial distribution and long-term changes in the surface biodiversity of diatoms, dinoflagellates, and copepods (Fig. 1)[23,27,28]. The analysis reveals consistent increases in biodiversity across an extensive area of the North Atlantic, supporting the hypothesis that ocean warming is enhancing extratropical biodiversity[33,34]. Anticipated by models originating from the MacroEcological Theory on the Arrangement of Life (METAL)[33], similar increases in biodiversity have also been observed for copepods28 and fish[35].

We investigated long-term and spatial changes in the annual biodiversity patterns of three taxonomic groups (Figs. 2 and 3). The observed trends in annual biodiversity patterns for diatoms and dinoflagellates showed an earlier onset in spring and a prolonged offset in late summer, indicating a longer annual duration of the high-biodiversity period in response to increasing temperature, particularly in the North Sea and the Northwest Atlantic. The observed long-term trends and spatial differences in annual biodiversity patterns in the four studied systems (Fig. 2) were also in agreement with theoretical (METAL-based) predictions8. For example, the diminution in diatom biodiversity observed in the Bay of Biscay suggests that the same patterns may be anticipated in the North Sea if temperature continues to rise (Fig. 2c-d). However, we note that we did not separate in this study oblate(i.e. diameter > height) and prolate (i,e, diameter < height) diatoms despite different phenologies and responses to climate change[31]. Although a decrease has been observed for oblates in the region, prolates have increased in summer because the latter are better adapted to stratified and nutrient-poor environments, owing to their cell elongation, which (i) gives them an advantage in low-turbulent environments by reducing their sinking rate or (ii) facilitates the absorption of nutrients through an increase in the surface to volume ratio[31]. For dinoflagellates, processes may be more complex because the North Sea may exhibit different patterns

than the Bay of Biscay. Indeed, North Sea dinoflagellates exhibited a decline in summer biodiversity, which is associated with increased thermal stratification and a longer duration of summers in this region[36], reducing productivity[23,37]. Based on our results that show latitudinal shifts in annual biodiversity patterns (Fig. 2), further increases in summer biodiversity may be anticipated for the North-East Atlantic with future climate warming.

We found a long-term increase in copepod biodiversity associated with a rise in the annual duration of the high-biodiversity period. These shifts agree with observed changes in copepod communities, which transitioned from a dominance of larger, herbivorous species capable of diapause with high summer abundance to smaller, carnivorous, and detritivorous species, characterised by shorter development times and increased autumn abundance in the North Sea[32]. Our findings of an absence of an increase in summer copepod biodiversity in the south-European basin should be interpreted with caution because of a lack of information on subtropical species south of the main area covered by the CPR survey. This drawback may also affect dinoflagellates but not diatoms, because their biodiversity diminishes towards subtropical regions[27].

The increase in biodiversity observed for the three taxonomic groups has been linked to warming and changes in nutrient concentration[38], which tend to favour smaller plankton species and may lead to a reduction in the size and biomass of higher trophic levels[39,40]. The restructuring of plankton size spectra may also alter the balance between nutrient recycling and export, impacting the efficiency of the biological carbon pump[29,41]. From an economic perspective, projected decreases in North Atlantic carbon sequestration may then trigger substantial losses, in terms of mitigation (~170 to 3,000 billion USD) and social costs (~23 to 401 billion USD)[42].

Phenology is a sensitive indicator of climate warming because recruitment success at higher trophic levels depends on the match between prey availability and predator demand10. Long-term plankton monitoring has revealed that many species are exhibiting an earlier phenology with rising temperatures[10], but such an analysis has never been applied to biodiversity. Our analysis has revealed similar shifts at a community level, highlighting an altered annual duration of the high biodiversity period for diatoms and dinoflagellates. The two groups exhibited earlier spring onsets and peaks as well as higher biodiversity later into summer, expanding the high biodiversity duration by up to 20 days [6.9; 18.2%] in the coldest regions (Fig. 2 and 3). Shifts were also observed for copepods, e.g. the North Sea, with an offset of high biodiversity by up to 12 days [8.29; 14.71], later in 2002-2022 compared with 1965-1985 (Fig. 3, Supplementary Table S2). Asch et al.[43] have provided compelling evidence that spring blooms at high latitudes (i.e. above 40°N) may occur on average 16 days earlier under an RCP8.5 scenario, with biological extreme events defined as >30 days of mismatch between prey and consumers leading to fish recruitment failure. Although it is difficult to know the extent to which these shifts may decouple trophic interactions, these projections are similar to the rate of shifts we found in the North Atlantic for the three plankton groups. It is likely that the shifts in annual biodiversity patterns will affect higher trophic levels such as fish, triggering trophic mismatch between predators and their prey[44].

Ferreira et al.[45] already showed that nearly a quarter of historical North Sea herring recruitment was explained by overlap with copepods and phytoplankton dynamics, illustrating the demographic sensitivity of fish populations to subtle timing shifts. Long-term observations in the Barents Sea further highlight such trophic linkages, with climate-driven fluctuations in copepod abundance and advection patterns driving inverse relationships between zooplankton biomass and capelin stocks, a key planktivorous fish[46].

We show that a major shift in annual biodiversity patterns has occurred throughout the North Atlantic, which suggests that important shifts in the phenology of species may be under way. Because biodiversity is a key ecosystem property that captures emerging community-level dynamics that affect ecosystem stability, energy transfer, and resilience, such changes may have potential consequences for regulating (e.g. carbon cycle)[29] and provisioning services[41]. Species richness alone is not sufficient to fully capture community dynamics, however, as a shift in species composition may also occur without changes in overall richness[33]. This underscores the need for complementary analyses of community composition but also highlights the need to maintain and reinforce marine plankton monitoring programmes to rapidly detect biological shifts at a time of an accelerating rise in global temperature[47].

Materials and Methods

Biological datasets

Plankton abundance data originated from the Continuous Plankton Recorder (CPR) survey, a long-term programme dedicated to the systematic monitoring of plankton on a monthly basis within the North Atlantic Ocean and its surrounding seas since 1931. We used data from 1958 when the methods were standardised. The methodological approach involves the deployment of a high-speed plankton recorder, towed behind merchant vessels at a depth ranging approximately from 7 to 10 meters[48]. Each recorded abundance value corresponds to the quantification of cells per CPR sample, which represents an approximate filtration volume of 3 m3 of seawater[49].

Diatoms and dinoflagellates constitute the phytoplankton components selected for this study. These two groups play key roles in pelagic food webs but differ in several fundamental ways: dinoflagellates are motile, using flagella to move, whereas diatoms have non-motile siliceous cell walls. Additionally, diatoms are strictly autotrophic while dinoflagellates can adopt mixotrophic feeding strategies. Seasonality further differentiates these groups, with each contributing to the food web at different times of the year[50]. Due to their position at the base of the food chain, both are highly responsive to environmental change. It is important to recognise that the CPR tends to selectively sample certain diatom and dinoflagellate taxa, particularly larger or spikier species, meaning smaller, more dominant taxa commonly found in bottle samples may be underrepresented[19]. Despite these limitations, the CPR sampling method has been consistent across time and regions, making comparisons over time and space reliable[51].

Copepods were selected as the zooplankton component for this study, as they are one of the most effectively sampled taxa by the CPR, often dominating zooplankton populations[52].

In this study, we used the abundance data collected for 46 copepod species, 26 dinoflagellate species and 45 diatom species (Supplementary Table S1). These species were selected based on their documented spatial distributions and because they are well sampled by the CPR survey[53]. To focus on this CPR survey area we restricted our study to 45°N-70°N and 100°W-40°E (Supplementary Fig. S1).

Environmental variables

The surface values of eight environmental parameters were linked to each CPR sample prior to the modelling of species abundance:

1. Bathymetry data were obtained from the GEBCO2021 Grid, downloaded from the General Bathymetric Chart of the Oceans (GEBCO) website (https://www.gebco.net/data_and_products/gridded_bathymetry_data/#global)[54]

2. Potential Temperature (Toa) and 3. Mixed Layer Depth (MLD) from the Global Ocean Reanalysis System version 5 (ORAS5)[55] were downloaded monthly (1958-2022) at a resolution of 0.25° for depths up to 10 meters.

4. Photosynthetically Active Radiation (PAR) originated from the Daily PAR product in depth retrieved at a resolution of 0.25° since 1958 for depths up to 10 meters[22].

Macronutrients (5. nitrate, 6. phosphate and 7. silicate) and 8. Chlorophyll-a (Chla) data were downloaded monthly (1958-2022) from the Coupled Model Intercomparison Project Phase 6 (CMIP6)[56] at a resolution of 1° for depths up to 10 meters. Data were spatially interpolated on a 0.25° latitude × 0.25° longitude grid and linearly interpolated to daily intervals. The simulations used were from IPSL-CM6A-LR, covering the period 1850-2014 (historical simulation) and 2015-2022 (future projection, modelled with the Shared Socioeconomic Pathways 585, corresponding to high radiative forcing by 2100)[57].

Modelling species richness: Environmental String Model

The reanalysis of the CPR data at high spatial and temporal resolution was carried out by means of the Environmental String Model (ESM)[20]. This new Ecological Niche Model (ENM) uses the concept of an environmental string (ES) to elucidate species-environment relationships and facilitate the characterisation of the multidimensional niche space, as per Hutchinson's niche theory[58], into two dimensions. An environmental string is defined as a composite representation of environmental parameters that preserves local relationships among variables, defined as environmental nodes. The model aims to estimate the abundance of unknown environmental strings or Target Environmental

Strings (TES) by using each ES within a Target Zone (TZ). Each node of an ES must be located in the TZ to contribute to the calculation of abundance associated with the TES. The closer an ES is to the TES, the higher its weight in the estimate. ESs with significant overlap in the TZ are used, while others are excluded; this also enables local relationships among variables to be considered. The abundance estimate becomes more reliable as more ESs are considered. Full mathematical details are in Beaugrand (2024)[20] and Castant et al. (2024)[22].

Different combinations of environmental factors were used within the ESM to model phytoplankton or zooplankton species in depth, based on ecological mechanisms governing plankton distribution in the water column. For phytoplankton species, MLD, Toa, Nitrates (NO_3), Phosphates (PO_4) and Silicates (Si) were used in the ESM. For zooplankton species, Toa, PAR, Chla and Bathymetry were used in the ESM. To refine the outputs, a bathymetric linear filter, where the preferred depth ranges for each species was determined from the visual inspection of the CPR plankton atlas[53], was applied for phytoplankton abundances, and a smoothing process using a linear function incorporating data from the preceding 20 days was applied for zooplankton abundances. Then, a first-order asymmetrical moving average was applied to integrate the upper 10 meters of depth for each species. A sketch diagram of the methodology is presented in supplementary Fig. S4. Other parameters used in the model initialization and sensitivity analyses are fully described in Castant et al. (2025)[21]. The spatial distribution of taxonomic richness was then computed at each available depth using a 4D species matrix. For this analysis, the abundance of species was computed between 0 and 10 m and then converted into presence-absence using a threshold of 0.1 (i.e., abundance > 0.1 means an occurrence). We then summed the presence of all copepod, diatom and dinoflagellate species to compute daily species richness as a measure of biodiversity.

The final products at the end of the procedure were a reanalysed species richness for the three taxonomic groups within a matrix of 101 Latitudes × 561 Longitudes × 23741 Days (365 days × 65 years, 1958-2022).

Analyses

Modelling and data analyses were conducted using MATLAB (2023). The mean species richness of the three taxonomic groups is mapped for surface waters over the period 1958-2022 (Fig. 1). Long-term trends (1958-2022) in species richness are assessed using a Kendall test[59,60]. This non-parametric test returns statistics after comparing every value in a time-series to each of the preceding ones. If the value at t+1 is higher than the value at t (t denotes a given year here), the pairwise comparison is assigned the value of 1. In cases where it is lower, it is assigned the value of -1, with 0 being assigned when there is no difference between values. The sum of all these types of pairwise comparisons for the time series produces Kendall's τ statistics. The sign of the test reveals the direction of the trend. The magnitude of the statistics is directly proportional to the strength of the trend. A p-value < 0.05 is set here to maintain significant monotonic trends. The total areas and associated percentages of significant increase and

decrease in species richness were computed to quantify the spatial extent of significant biodiversity change across the North Atlantic.

Long-term changes were then examined focussing on four distinct regions, selected for their contrasting hydrographic regimes along a latitudinal thermal gradient (Supplementary Fig. S1): (i) the North-West Atlantic (NWA, Longitude 45°W-40°W Latitude 55°N-58°N, mean temperature of 5.95 °C); (ii) the North-East Atlantic (NEA, Longitude 20°W-3°W Latitude 60°N-63°N, mean temperature of 9.27 °C); (iii) the North Sea (NS, Longitude 3°W-8°E Latitude 55°N-60°N, mean temperature of 9.89 °C); and (iv) the Bay of Biscay (BSC, Longitude 12°W-4°W Latitude 45°N-47°N, mean temperature of 14.97 °C). A 30-day symmetric moving average is applied to each group within each region to smooth the data and provide a clearer visualization of the daily changes, and the results are compared with changes in daily temperature in the region (Fig. 2). Daily trends in species richness were then explored by regions and by computing the Kendall τ coefficients (p-value < 0.05) for each calendar day within each of the three taxonomic groups.

Indicators, that were originally derived from phenology research to measure changes in annual biodiversity patterns, were computed for each year and group in each of four distinct regions based on the cumulative sums of anomalies method[61] (Supplementary Fig. S2). We derived five indicators of biodiversity (i.e. plankton richness): Annual Duration of a high-richness period, Onset of the high-richness period, Offset of the high-richness period, day of Maximum Annual Richness (MAR), and Mean annual richness. Daily species richness time series were first standardised and averaged across years, regions and groups to compute a climatology. From this climatology, we calculated the cumulative sum of anomalies (i.e., deviations from the mean climatology) and subsequently derived its gradient. The points where the gradient crossed zero (i.e., where the richness time series switched sign) were used to define a threshold value of high species richness. Yearly onset and offset values were then determined as the first and last days when standardised richness reaches this threshold. Duration was calculated as the number of days between onset and offset, MAR was identified for each year as the day of peak richness, and mean annual richness was computed each year across the full cycle (Supplementary Fig. S3).

Finally, we quantified phenological shifts for each group, region, and indicator by comparing two 20-year periods, 1965-1985 (relatively cold in a negative Atlantic Multidecadal Variability or AMV phase, ~8,82°C) and 2002-2022 (relatively warm in a positive AMV phase, ~9,14°C, Fig. 3). To assess whether indicators differed significantly between periods, we employed a bootstrap resampling framework (10,000 iterations) combined with the Mann-Whitney U test[62]. We first computed the observed Mann-Whitney U statistics from the original data. Then, both samples were resampled in each bootstrap iteration with replacement under a null distribution defined by centering the data using the Hodges-Lehmann estimator[63], ensuring that the bootstrap null distribution reflects differences in central tendency without assuming symmetry. The Mann-Whitney U statistic is recalculated on the resampled data to generate a bootstrap null distribution, against which the observed statistics were compared to calculate two-sided p-values (significance set at p-value < 0.05). In parallel, we estimated 95% confidence intervals for group medians from the bootstrap distributions (2.5th, 50th and 97.5th percentiles) to provide robust

uncertainty estimates. Median differences were calculated to determine the direction of the shifts, with associated percent changes (with 95% confidence intervals), expressed relative to 1965-1985 values, computed for duration and mean annual richness.

Declarations

Acknowledgements

The authors are grateful to the Centre National d'Etudes Spatiales (CNES) and l'Université du Littoral Côte d'Opale (ULCO) for co-funding the doctoral scholarship of J.C. We also thank the CPER programme IDEAL and the graduate school IFSEA that benefits from a France 2030 ANR-21 EXES-0011 from the French National Research Agency, under the Investments for the Future Programme, and by the ULCO and the Institut des Sciences de la Mer et du Littoral (ISML). This work was also funded by the TOSCA/CNES program. Finally, some experiments presented in this paper were carried out using the CALCULCO computing platform, supported by SCoSI/ULCO (Service COmmun du Système d'Information de l'ULCO).

Contributions

J.C., G.B., and V.V. conceived the study. J.C. curated, processed, and analysed the data. J.C. and G.B. wrote the manuscript. V.V. and P.C.R. edited the manuscript text and figures. All authors discussed the results and approved the final manuscript.

Competing interests

The authors declare no competing interests.

Data availability

The data that support the findings of this study are available from the authors on reasonable request.

References

1. McQuatters-Gollop, A. *et al.* Assessing the state of marine biodiversity in the northeast atlantic. *Ecol. Indic.* **141**, 109148 (2022).
2. Passow, U. & Carlson, C. A. The biological pump in a high CO2 world. *Mar. Ecol. Prog. Ser.* **470**, 249–271 (2012).
3. Lima-Mendez, G. *et al.* Determinants of community structure in the global plankton interactome. *Science* **348**, 1262073 (2015).

4. Kulk, G. *et al.* Primary production, an index of climate change in the ocean: satellite-based estimates over two decades. *Remote Sens.* **12**, 826–852 (2020).
5. Luczak, C., Beaugrand, G., Jaffré, M. & Lenoir, S. Climate change impact on balearic shearwater through a trophic cascade. *Biol. Lett.* **7**, 702–705 (2011).
6. de Vargas, C. *et al.* Plankton planet: a frugal, cooperative measure of aquatic life at the planetary scale. *Front. Mar. Sci.* **9**, 0–17 (2022).
7. Heneghan, R. F., Everett, J. D., Blanchard, J. L., Sykes, P. & Richardson, A. J. Climate-driven zooplankton shifts cause large-scale declines in food quality for fish. *Nat. Clim. Change* **13**, 470–477 (2023).
8. Beaugrand, G. & Kirby, R. R. How do marine pelagic species respond to climate change? Theories and observations. *Annu. Rev. Mar. Sci.* **10**, 169–197 (2018).
9. Chivers, W. J., Edwards, M. & Hays, G. C. Phenological shuffling of major marine phytoplankton groups over the last six decades. *Divers. Distrib.* **26**, 536–548 (2020).
10. Edwards, M. & Richardson, A. J. Impact of climate change on marine pelagic phenology and trophic mismatch. *Nature* **430**, 881–884 (2004).
11. Kwon, E. Y. *et al.* Nutrient uptake plasticity in phytoplankton sustains future ocean net primary production. *Sci. Adv.* **8**, eadd2475 (2022).
12. Cael, B. B., Cavan, E. L. & Britten, G. L. Reconciling the size-dependence of marine particle sinking speed. *Geophys. Res. Lett.* **48**, e2020GL091771 (2021).
13. Serra-Pompei, C. *et al.* Linking plankton size spectra and community composition to carbon export and its efficiency. *Global Biogeochem. Cycles* **36**, e2021GB007275 (2022).
14. Corona, S. *et al.* Long-term shifts in phenology, thermal niche, population size, and their interactions in marine pelagic copepods. *Limnol. Oceanogr.* **69**, 482–497 (2024).
15. Honda, I. A. *et al.* Shifting phenology as a key driver of shelf zooplankton population variability. *Limnol. Oceanogr.* **70**, 178–188 (2025).
16. Henson, S. A., Cael, B. B., Allen, S. R. & Dutkiewicz, S. Future phytoplankton diversity in a changing climate. *Nat. Commun.* **12**, 5372 (2021).
17. Álvarez, E., Occhipinti, G., Cossarini, G., Solidoro, C. & Lazzari, P. Modeling plankton diversity in a coupled optical-biogeochemical ocean framework. *Front. Ecol. Evol.* **13**, 0–13 (2025).
18. Isbell, F. *et al.* Expert perspectives on global biodiversity loss and its drivers and impacts on people. *Front. Ecol. Environ.* **21**, 94–103 (2023).
19. Richardson, A. J. *et al.* Using continuous plankton recorder data. *Prog. Oceanogr.* **68**, 27–74 (2006).
20. Beaugrand, G. An ecological niche model that considers local relationships among variables: the environmental string model. *Ecosphere* **15**, e70015 (2024).
21. Castant, J., Vantrepotte, V., Thibault, H. & Beaugrand, G. Long-term changes in depth distribution and phenology of four north atlantic plankton species. *Mar. Ecol. Prog. Ser.* **771**, 33–53 (2025).

22. Castant, J., Vantrepotte, V., Frouin, R. & Beaugrand, G. Comprehensive gridded dataset of photosynthetically active radiation in the upper ocean from 1958 to 2022. *Remote Sens. Environ.* **311**, 114305 (2024).
23. Holland, M. M. *et al.* Major declines in NE atlantic plankton contrast with more stable populations in the rapidly warming north sea. *Sci. Total Environ.* **898**, 165505 (2023).
24. Beaugrand, G., Reid, P. C., Ibañez, F. & Planque, B. Biodiversity of north atlantic and north sea calanoid copepods. *Mar. Ecol. Prog. Ser.* **204**, 299–303 (2000).
25. Kléparski, L., Beaugrand, G. & Edwards, M. Plankton biogeography in the north Atlantic Ocean and its adjacent seas: species assemblages and environmental signatures. *Ecol. Evol.* **11**, 5135–5149 (2021).
26. Bruera, R., Curbelo, J., García-Sánchez, G. & Mancho, A. M. Mixing and geometry in the north atlantic meridional overturning circulation. *Geophys. Res. Lett.* **50**, e2022GL102244 (2023).
27. Barton, A. D., Irwin, A. J., Finkel, Z. V. & Stock, C. A. Anthropogenic climate change drives shift and shuffle in north atlantic phytoplankton communities. *Proc. Natl. Acad. Sci.* **113**, 2964–2969 (2016).
28. Kléparski, L. *et al.* Ocean climate and hydrodynamics drive decadal shifts in northeast atlantic dinoflagellates. *Global Change Biol.* **30**, e17163 (2024).
29. Beaugrand, G., Edwards, M. & Legendre, L. Marine biodiversity, ecosystem functioning, and carbon cycles. *Proc. Natl. Acad. Sci.* **107**, 10120–10124 (2010).
30. Melbourne-Thomas, J. *et al.* Poleward bound: adapting to climate-driven species redistribution. *Rev. Fish Biol. Fish.* **32**, 231–251 (2022).
31. Kléparski, L., Beaugrand, G., Edwards, M. & Ostle, C. Phytoplankton life strategies, phenological shifts and climate change in the north Atlantic Ocean from 1850 to 2100. *Global Change Biol.* **29**, 3833–3849 (2023).
32. Deschamps, M. M. *et al.* Major shift in the copepod functional community of the southern north sea and potential environmental drivers. *ICES J. Mar. Sci.* **81**, 540–552 (2024).
33. Beaugrand, G., Edwards, M., Raybaud, V., Goberville, E. & Kirby, R. R. Future vulnerability of marine biodiversity compared with contemporary and past changes. *Nat. Clim. Change* **5**, 695–701 (2015).
34. Ibarbalz, F. M. *et al.* Global trends in marine plankton diversity across kingdoms of life. *Cell* **179**, 1084-1097.e21 (2019).
35. Hiddink, J. G. & Hofstede, R. T. Climate induced increases in species richness of marine fishes. *Global Change Biol.* **14**, 453–460 (2008).
36. Bopp, L. *et al.* Multiple stressors of ocean ecosystems in the 21st century: projections with CMIP5 models. *Biogeosciences* **10**, 6225–6245 (2013).
37. Edwards, M., Beaugrand, G., Kléparski, L., Hélaouët, P. & Reid, P. C. Climate variability and multi-decadal diatom abundance in the northeast atlantic. *Commun. Earth Environ.* **3**, 1–8 (2022).
38. Di Pane, J., Wiltshire, K. H., McLean, M., Boersma, M. & Meunier, C. L. Environmentally induced functional shifts in phytoplankton and their potential consequences for ecosystem functioning.

Global Change Biol. **28**, 2804–2819 (2022).

39. Tittensor, D. P. *et al.* Next-generation ensemble projections reveal higher climate risks for marine ecosystems. *Nat. Clim. Change* **11**, 973–981 (2021).
40. Atkinson, A. *et al.* Steeper size spectra with decreasing phytoplankton biomass indicate strong trophic amplification and future fish declines. *Nat. Commun.* **15**, 381–392 (2024).
41. Benedetti, F. *et al.* Major restructuring of marine plankton assemblages under global warming. *Nat. Commun.* **12**, 5226 (2021).
42. Barange, M. *et al.* The cost of reducing the north Atlantic Ocean biological carbon pump. *Front. Mar. Sci.* **3**, 0–10 (2017).
43. Asch, R. G., Stock, C. A. & Sarmiento, J. L. Climate change impacts on mismatches between phytoplankton blooms and fish spawning phenology. *Global Change Biol.* **25**, 2544–2559 (2019).
44. Durant, J. M. *et al.* Extension of the match-mismatch hypothesis to predator-controlled systems. *Mar. Ecol. Prog. Ser.* **474**, 43–52 (2013).
45. Ferreira, A., Brotas, V., Palma, C., Borges, C. & Brito, A. C. Assessing phytoplankton bloom phenology in upwelling-influenced regions using ocean color remote sensing. *Remote Sens.* **13**, 675–703 (2021).
46. Skjoldal, H. R. Size-fractioned zooplankton biomass in the barents sea ecosystem: changes during four decades of warming and four capelin collapses (1980–2020). *ICES J. Mar. Sci.* **81**, 512–525 (2024).
47. Beaugrand, G., Reid, P. & Conversi, A. Acceleration of changes in global surface temperature after the Earth system has crossed a tipping point. *Clim. Res.* **95**, 1–17 (2025).
48. Batten, S. D. *et al.* CPR sampling: the technical background, materials and methods, consistency and comparability. *Prog. Oceanogr.* **58**, 193–215 (2003).
49. Jonas, T. D., Walne, A., Beaugrand, G., Gregory, L. & Hays, G. C. The volume of water filtered by a continuous plankton recorder sample: the effect of ship speed. *J. Plankton Res.* **26**, 1499–1506 (2004).
50. McQuatters-Gollop, A., Raitsos, D., Edwards, M. & Attrill, M. Spatial patterns of diatom and dinoflagellate seasonal cycles in the NE atlantic ocean. *Mar. Ecol. Prog. Ser.* **339**, 301–306 (2007).
51. McQuatters-Gollop, A. *et al.* The continuous plankton recorder survey: how can long-term phytoplankton datasets contribute to the assessment of good environmental status? *Estuarine Coastal Shelf Sci.* **162**, 88–97 (2015).
52. Beaugrand, G., Reid, P. C., Ibañez, F., Lindley, J. A. & Edwards, M. Reorganization of north atlantic marine copepod biodiversity and climate. *Science* **296**, 1692–1694 (2002).
53. Beaugrand, G. Continuous plankton records: plankton atlas of the north Atlantic Ocean (1958–1999). I. Introduction and methodology. *Mar. Ecol. Prog. Ser.* 3–10 (2004) doi:10.3354/mepscpr003.
54. Gebco. GEBCO_2021 grid - a continuous terrain model of the global oceans and land. *British Oceanographic Data Centre*

https://www.bodc.ac.uk/data/published_data_library/catalogue/10.5285/c6612cbe-50b3-0cff-e053-6c86abc09f8f/ (2021) doi:10.5285/c6612cbe-50b3-0cff-e053-6c86abc09f8f.

55. Zuo, H., Balmaseda, M. A., Tietsche, S., Mogensen, K. & Mayer, M. The ECMWF operational ensemble reanalysis–analysis system for ocean and sea ice: a description of the system and assessment. *Ocean Sci.* **15**, 779–808 (2019).
56. Eyring, V. *et al.* Overview of the coupled model intercomparison project phase 6 (CMIP6) experimental design and organization. *Geosci. Model Dev.* **9**, 1937–1958 (2016).
57. O'Neill, B. C. *et al.* The roads ahead: narratives for shared socioeconomic pathways describing world futures in the 21st century. *Global Environ. Change* **42**, 169–180 (2017).
58. Hutchinson, G. E. Concluding remarks. Cold spring harbor symposia on quantitative biology. Volume 22. **22**, 415–427 (1957).
59. Bedford, J. *et al.* Lifeform indicators reveal large-scale shifts in plankton across the north-west european shelf. https://doi.org/10.1111/gcb.15066 (2020) doi:10.1111/gcb.15066.
60. Burkey, J. A non-parametric monotonic trend test computing mann-kendall tau, tau-b, and sen' slope written in mathworks-MATLAB implemented using matrix rotations (2006). http://www.mathworks.com/matlabcentral/fileexchange/authors/23983
61. Kournopoulou, A. *et al.* Atlas of phytoplankton phenology indices in selected eastern Mediterranean marine ecosystems. *Sci. Rep.* **14**, 9975 (2024).
62. Mann, H. B. & Whitney, D. R. On a test of whether one of two random variables is stochastically larger than the other. *Ann. Math. Stat.* **18**, 50–60 (1947).
63. Hodges, J. L. & Lehmann, E. L. Estimates of location based on rank tests. *Ann. Math. Stat.* **34**, 598–611 (1963).

Figures

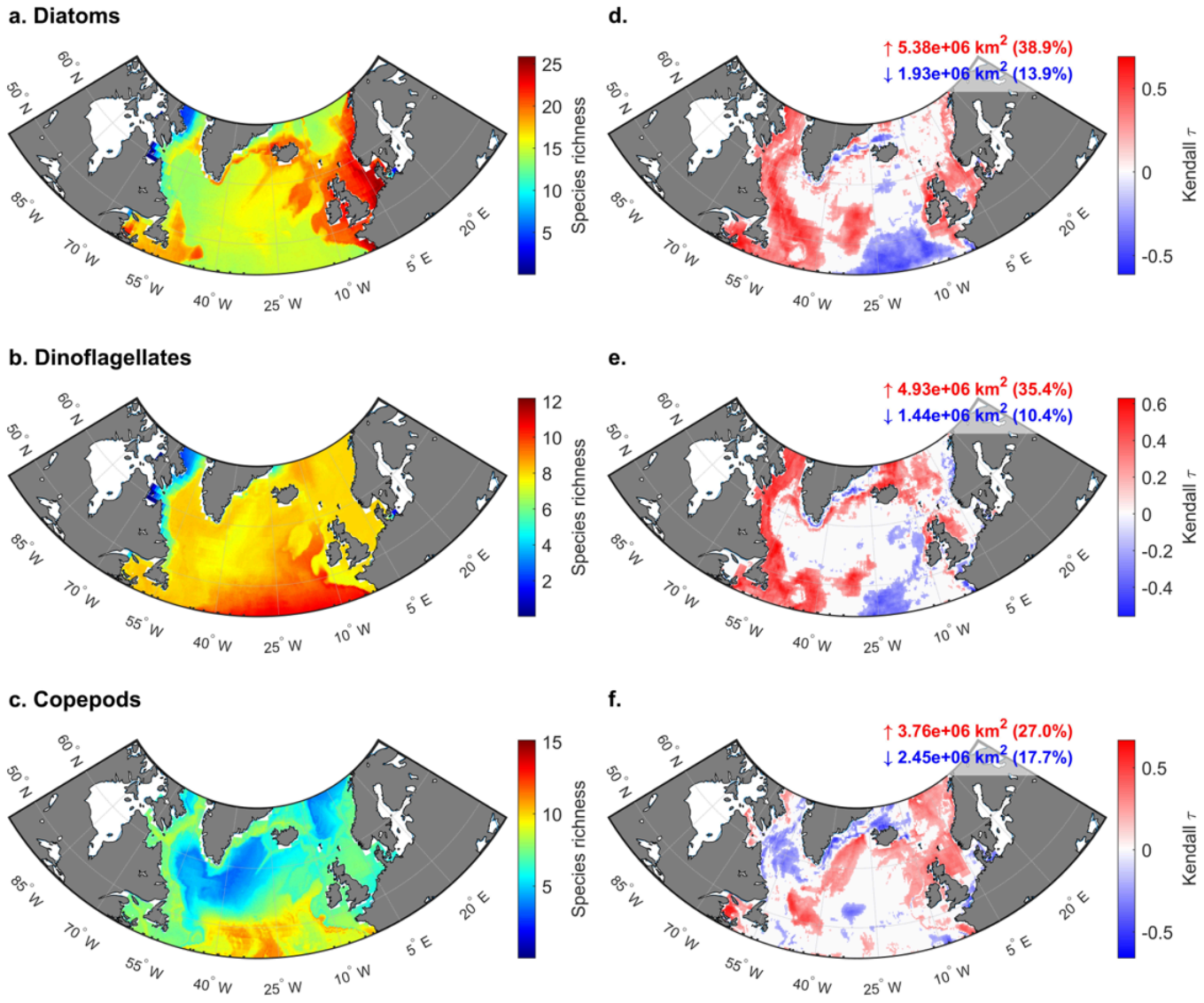


Figure 1

Reanalysed North Atlantic surface (0-10m) maximum species richness (expressed as the average of the yearly maximum number of species from 1958-2022, a-c) and Kendall coefficient τ to assess the temporal trend in yearly means (d-f), comprising (a, d) Diatoms, (b, e) Dinoflagellates and (c, f) Copepods. The Kendall τ coefficient assesses the sign and strength of the changes in species richness. A positive trend (red) denotes a significant (p-value < 0.05) increase in biodiversity and a negative trend (blue) shows a decrease. An absence of colour denotes no significant long-term changes in biodiversity. The red and blue annotations in panels (d-f) indicate the total areas and associated percentages of significant increase and decrease in species richness, respectively.

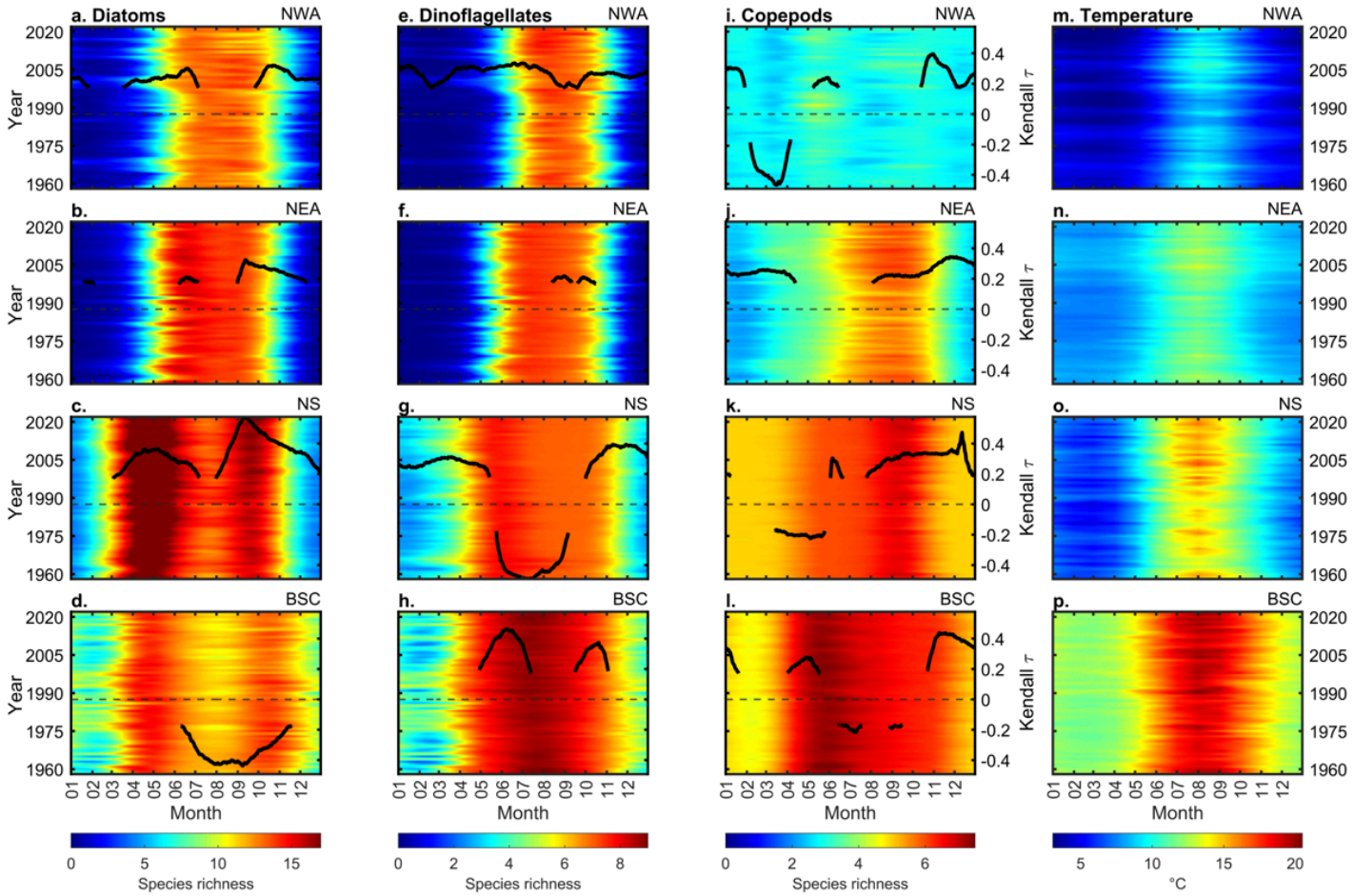


Figure 2

Reanalysed long-term changes (1958-2022) in mean daily biodiversity (i.e. species richness, 0-10m) and associated Kendall τ (black lines) for diatoms (a-d), dinoflagellates (e-h) and copepods (i-l) with associated temperature (m-p) over the North-West Atlantic (NWA, mean temperature: 5.95°C, bathymetry: 3302 m [2589-3493 m], a, e, i, m); the North-East Atlantic (NEA, mean temperature: 9.27°C, bathymetry: 1244 m [16-2735 m], b, f, j, n), the North-Sea (NS, mean temperature: 9.89°C, bathymetry: 95 m [6-359 m], c, g, k, o) and the Bay of Biscay (BSC, mean temperature:14.97°C, bathymetry: 4133 m [124-5032 m], d, h, l, p). A positive or a negative value of the Kendall coefficient denotes a long-term increase or a decrease in biodiversity, respectively. See the mapping of the different selected regions in Supplementary Fig. S1.

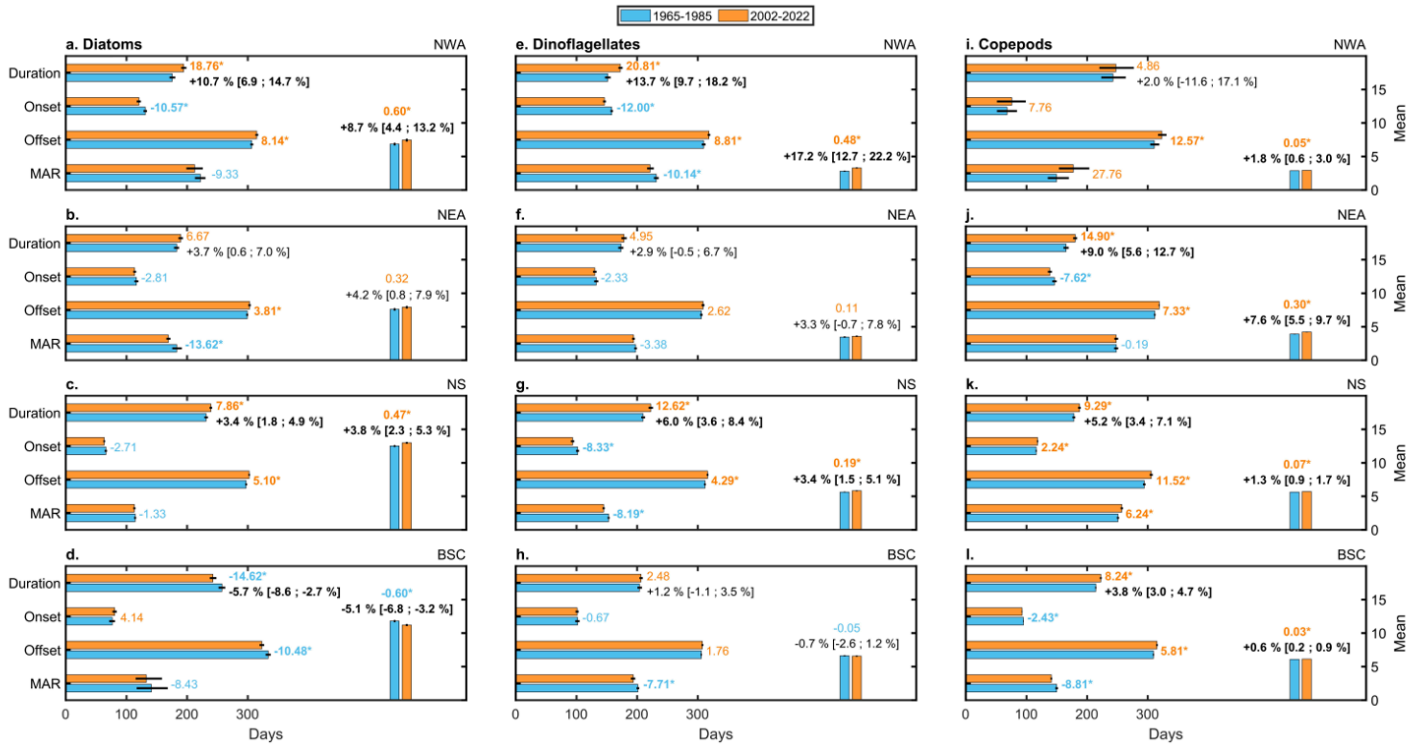


Figure 3

Estimates of changes in annual biodiversity (species richness) patterns for diatoms (a-d), dinoflagellates (e-h), and copepods (i-l) across four regions: North-West Atlantic (NWA), North-East Atlantic (NEA), North Sea (NS), and Bay of Biscay (BSC). Medians and confidence intervals (2.5th and 97.5th percentiles) for five indicators were calculated for two time periods (1965-1985, blue bars; 2002-2022, orange bars): annual Duration of the period with a high species richness, Onset, Offset, day of Maximum Annual Richness (MAR) (horizontal bars at the left side) and mean annual richness (vertical bars at the right side). Numbers next to the bars show the difference of medians between periods, with the colour indicating which period is higher. Significant differences between periods are assessed with a Mann-Whitney U test and highlighted in bold with an asterisk (*). The 95% confidence intervals for these differences are presented in Supplementary Table S2. Associated percent changes (with 95% confidence intervals), expressed relative to 1965-1985 values, are shown for duration and mean annual richness.

Supplementary Files

This is a list of supplementary files associated with this preprint. Click to download.

- SupplementaryMaterials.docx